UNIVERSIDAD DISTRITAL
FRANCISCO JOSÉ DE CALDAS

Colombia FORESTAL

Publicación de la Facultad del Medio Ambiente y Recursos Naturales–Proyecto Curricular de Ingeniería Forestal
revistas.udistrital.edu.co/ojs/index.php/colfor/index

https://doi.org/10.14483/2256201X.23488

RESEARCH ARTICLE

ISSN 0120-0739 • e-ISSN 2256-201X

Effects of Adding Pretreated Chestnut (*Bertholletia excelsa*) Mesocarp Fibers to Fiber-Cement Boards

Efectos de la adición de fibras pretratadas de mesocarpio de castaño (*Bertholletia excelsa*) a tableros de fibrocemento

Carlos Enrique Mori-Seminario[a], Héctor Enrique Gonzáles-Mora[a], Julio André Gamarra-Bustamante[a], Aldo Joao Cárdenas-Oscanoa[a]

a Forest Industry Department, Faculty of Forest Sciences, Universidad Nacional Agraria La Molina. Lima, Perú.
Corresponding author

Received: April 26, 2025 **Accepted:** September 9, 2025

Citación: Mori-Seminario, C. E., Gonzáles-Mora, H. E., Gamarra-Bustamante, J. A., & Cárdenas-Oscanoa, A. J. (2026). Effects of adding pretreated chestnut (*Bertholletia excelsa*) mesocarp fibers to fiber-cement boards. *Colombia Forestal, 29*(1), e23488.
https://doi.org/10.14483/2256201X.23488

Highlighgts

- A soda pretreatment enhanced the mechanical properties of boards with 3% fiber.
- A NaOH treatment enhanced fiber adhesion to cement, improving mechanical properties.
- NaOH-treated fibers diminished water absorption in fiber-cement boards.
- The application of NaOH to the fibers resulted in a reduction of their holocellulose content.
- The produced boards comply with the national standard requirements for compression.

Abstract

Natural fibers have gained relevance due to their renewable nature, which makes them promising candidates as reinforcement materials. Chestnut (*Bertholletia excelsa*) mesocarp fibers have been found to be suitable for incorporation into fiber-cement boards. In this work, two types of boards were produced, with fiber contents of 3, 6, and 9%: one type used fibers pretreated in a 10% NaOH alkali solution, and the other one was left untreated. Comprehensive chemical and analytical assessments were carried out, accompanied by mechanical performance evaluations. The pretreatment reduced the fiber holocellulose content

by 5.32%. Incorporating chestnut fibers decreased the board density by up to 13%, regardless of the treatment. The most favorable outcomes regarding the reduction in thickness (up to 3.4% compared to the control group) were observed in samples containing 3% fiber. Notably, boards with pretreated fibers surpassed the Peruvian national standards by 10%. These results position chestnut mesocarp fibers as a promising reinforcement for fiber-cement boards and warrant further investigation.
Keywords: Chestnut (*Bertholletia excelsa*), fiber-cement board, mesocarp fibers, NaOH pretreatment

Resumen
Las fibras naturales han ganado relevancia por su carácter renovable, lo que las hace candidatas promisorias como materiales de refuerzo. Se ha encontrado que las fibras del mesocarpio de castaña (*Bertholletia excelsa*) son aptas para el uso en tableros de fibrocemento. En este trabajo se fabricaron dos tipos de tableros, con 3, 6 y 9% de fibra: uno de estos tipos utilizó fibras pretratadas en una solución alcalina al 10% de NaOH, y el otro se dejó sin tratar. Se realizaron evaluaciones químicas y analíticas, acompañadas por valoraciones de rendimiento mecánico. El pretratamiento redujo el contenido de holocelulosa de las fibras en un 5.32%. La incorporación de fibras disminuyó la densidad de los tableros hasta en un 13%, sin importar el tratamiento. Los mejores resultados en cuanto a la reducción de espesor (hasta 3.4% con respecto al grupo control) se observó en muestras con 3% de fibra. Cabe destacar que los tableros con fibras pretratadas superaron los estándares nacionales del Perú en un 10%. Estos resultados posicionan las fibras de mesocarpio de castaña como refuerzo para tableros de fibrocemento y requieren mayor estudio.
Palabras clave: Castaña (*Bertholletia excelsa*), tablero de fibrocemento, fibras de mesocarpio, pre-tratamiento de NaOH

INTRODUCTION

Throughout evolutionary history, various natural resources have been harnessed, with plant-based fibers holding particular significance. In the Amazon forest, for example, natural resources are prominent. While wood logging has been extensive, other resources remain largely underutilized. Natural fibers are fibrous polymeric composites derived from renewable resources, which are primarily composed of cellulose. Lignocellulosic fibers are natural fibers consisting of cellulose, hemicellulose, and lignin, predominantly containing 50-70% cellulose (Arango-Perez *et al*., 2023; Atúncar Vilela *et al*., 2024). These fibers offer notable benefits such as low density, high specific hardness, biodegradability, and availability. The most common plants from which fibers are extracted include flax, hemp, bamboo, sisal, and jute. Moreover, plant fibers can be classified morphologically based on their origin, *e.g.*, bast fibers (flax, jute, ramie, hemp, kenaf), leaves (sisal, pineapple, banana), seeds (cotton), fruit (coconut), straw (rice, corn), or others (bamboo, bagasse).

In Peru, chestnut fruit is a significant nontimber forest resource. Specifically, the chestnut *Bertollethia excelsa* is recognized as one of the most important nontimber forest products in the Madre de Dios region of southeastern Peru, with an annual seed demand exceeding 5 400 000 kg. Although this species' wood can serve various purposes, its fruit holds greater commercial value for its seed or edible endosperm. However, the extraction process of the endosperm yields substantial pericarp residues (exocarp, mesocarp, and endocarp) from the fruit. This exploitation generates significant waste, constituting roughly 76% of the entire fruit.

The chestnut fruit comprises 25% exocarp, 50% mesocarp, 1% endocarp, and 12% seed shells and edible endosperm; thus, 76% of the fruit is pericarp (Petrechen *et al*., 2019). The mesocarp features fibrous, sclereid, and vascular cell regions that are organized similarly to the composite materials. Integrating chestnut-mesocarp particles into various polypropylene matrices can significantly enhance the mechanical properties of the resulting biocomposite (Soares *et al*., 2023). In addition, the chestnut mesocarp is a lignocellulosic material with substantial potential for biocomposite production, offering impact and percolation resistance (Sonego *et al*., 2019). Therefore, it is essential to investigate the properties of mesocarp fibers to determine their suitability in strengthening the composite materials that are widely used in industry and construction.

In the realm of civil construction materials, fibers are incorporated to enhance mechanical performance, particularly by improving flexural properties and mitigating crack propagation in cement-based materials (Laverde *et al*., 2022). Using short plant fibers as internal reinforcement material increases the flexural and tensile strength of fiber-cement, as well as its toughness. In contrast, long fibers, when used as an external reinforcement, can enhance resistance and ductility (Laverde *et al*., 2022). Fiber-cement—more specifically fiber-reinforced cement (be it natural or synthetic)—is a composite material that can significantly boost the mechanical attributes and longevity of traditional cement-based products. Cement combined with lignocellulosic fibers generally falls into two categories: *fiber-reinforced cement* and *cement bonded with wood particles* (Hasan *et al*., 2022). These lignocellulosic composite materials are primarily utilized in construction, given their suitability for cladding panels, decorative purposes, renovation projects, environments with humid or hot climates, partitions, balconies, roofing, permanent structures, thermal insulation, specialized flooring, mobile homes, and acoustic barriers (Hasan *et al*., 2022; Hincapié Rojas *et al*., 2020). A variety of plant fibers have been investigated with the purpose of reinforcing cement matrices, including those derived from banana (Sales *et al*., 2022; Teixeira *et al*., 2020), sisal (Correia *et al*., 2018; Wei & Meyer, 2016), hemp and jute (Choi & Choi, 2021), coconut (Correia *et al*., 2018; Martinelli *et al*., 2023; Teixeira *et al*., 2020), sugarcane bagasse (Correia *et al*., 2018), curauá (Soltan *et al*., 2017), bamboo pulp (Campello *et al*., 2016), pine and eucalyptus pulp (Mármol & Savastano, 2017), and coffee husk (Teixeira *et al*., 2020). For instance, Gamarra *et al*. (2024) conducted an assessment of fiber-cement boards manufactured with mesocarp fibers from oil palm (*Elaeis guineensis* Jacq.). According to their results, boards containing 3% fiber demonstrated the most advantageous physical and mechanical characteristics, particularly in terms of water absorption and thickness swelling reduction, which is attributable to a higher density and reduced water absorption and porosity. Similarly, Fonseca *et al*. (2019) reported that composites reinforced with jute micro/nanofiber (*Corchorus* sp.) exhibit superior performance regarding their modulus of rupture (MOR) and their modulus of elasticity (MOE), even when subjected to natural weathering conditions.

Consequently, considering the potential of chestnut mesocarp, this research examined its application and performance as a reinforcing agent in fiber-cement production. In addition, we sought to assess the chemical properties of *B. excelsa* mesocarp fibers by measuring their extractives, holocellulose, and lignin levels in samples without pretreatment (NT) and with an alkaline pretreatment (T). This research also focused on determining density, water absorption, and swelling for physical characterization, as well as on assessing the static bending resistance and the reduction in thickness under compression, in order to understand the mechanical properties of the fiber-cement boards made with NT and T fibers.

MATERIALS AND METHODS

Chestnut-nut mesocarp fibers

The chestnut fruits used herein were sourced from the Madre de Dios Chestnut Growers Association (RONAP), which is located at the Alegría populated center in Las Piedras district, Tambopata province, Madre de Dios, Peru. A total of 22.5 kg of air-dried fruits were mechanically pressed using a Delfabro hydraulic press, model 15 Tn Foot 2 c (41030), with a pressure of 3.25 tons, to extract the mesocarp (Figure 1). The extracted mesocarp was then reduced to ~30 mm long pieces using a chisel and hammer. The material was subsequently divided into two groups. One group remained untreated (NT), while the other was subjected to an alkaline pretreatment (T) by soaking in a 10% NaOH solution for 24 h at room temperature (23 °C). The NaOH was prepared using sodium hydroxide pellets (Merck KGaA) dissolved in distilled water in the appropriate proportion.

The NT mesocarp fibers were ground in an electric knife mill with a 2-HP motor and sieved using 30-mesh (595 µm) and 40-mesh (400 µm) screens. The fraction retained on the 40-mesh screen was selected for use. The T samples were rinsed thoroughly with distilled water to neutralize the pH, and the fibers were then separated using a traditional Corona manual mill designed for high-hopper grains.

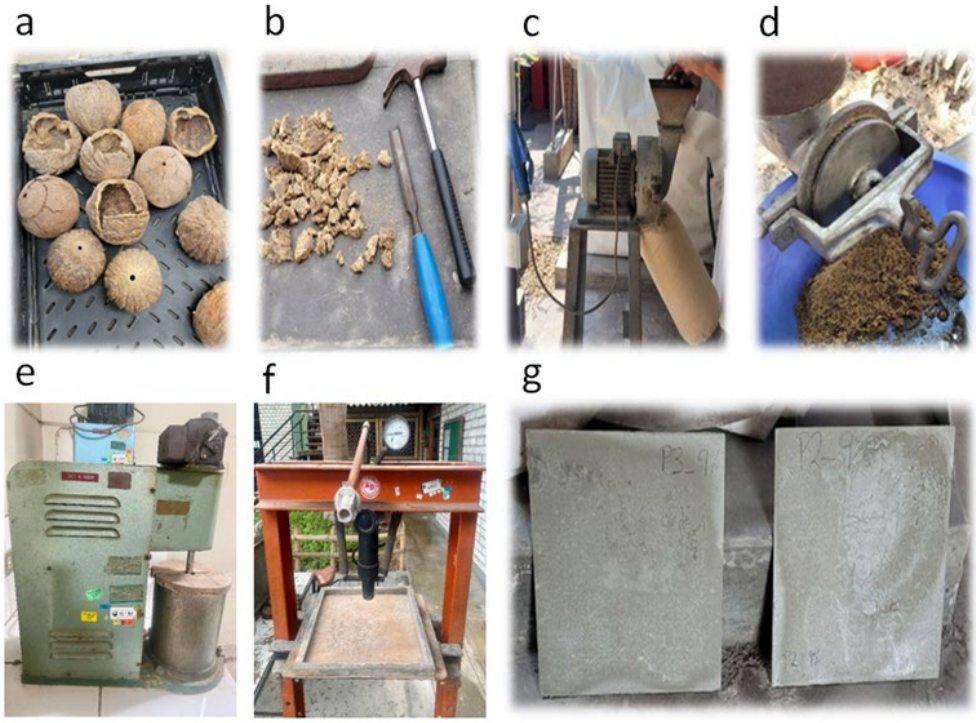

Figure 1. a) Pericarp of chestnut fruits; b) 30-mm long fiber fragments; c) grinding of chestnut fibers; d) fibrous material of the second group, obtained from the Corona manual grain mill; e) British pulp disintegrator; f) Delfabro 15 Tn Foot 2 c (41030) hydraulic press and 35 × 35 × 0.5 cm^3 wooden mold; g) fiber-cement boards.

Upon completing these procedures, both the NT and T mesocarp fibers were obtained. These fibers were then classified using a Bauer-McNett classifier according to the TAPPI-T 233 cm-06 standard.

Fiber-cement board production

The NT and T fibers were processed for 15 min in a British pulp evaluation apparatus (Mavis Engineering Ltd., Model No. 1215), followed by a 10 min immersion in a 4% calcium hydroxide ($Ca(OH)_2$) mineralizing solution. The $Ca(OH)_2$ solution was prepared by dissolving Cal Nieve (Martell brand) in mineral water at the specified concentration. After soaking, the fibers were removed, and the excess liquid was drained off.

Fiber-cement boards were produced using four different mass percentages of chestnut fiber: 0, 3, 6, and 9% for both NT and T fibers. The cement, fibers, and water were mixed in a Phillips HR 1456 mixer for 5 min. The water-to-cement ratio was maintained at 0.4:1.

The blended mixture was transferred into wooden molds measuring 35 × 35 × 0.5 cm^3 and pressed at 3 MPa for 24 h using a hydraulic press (Delfabro model 15 Tn Foot 2 c, 41030). Subsequently, the molds were placed in a shaded area at room temperature. For the first seven days, the samples were periodically sprayed with water to ensure proper curing. The boards were then allowed to complete the curing process for a total of 28 days at 23 °C (room temperature). After this curing period, test specimens were cut to the required dimensions using an angle grinder (Baukrer, 900 W, 11 000 rpm, 50/60 Hz). The final dimensions of the boards were 35 × 35 × 0.5 cm^3 (Figure 1).

Assessing the NT and T fibers

Chemical characterization

The chemical properties of the NT and T fibers were assessed according to the following standards. The contents of extractives soluble in alcohol and in distilled water were determined using TAPPI T 204 cm-07 and TAPPI T 207 cm-08, respectively. The ash content was determined as per the ASTM D 1762 standard (2013). The holocellulose content was determined according to TAPPI T 9 wd-75 via the Jayme-Wise method. Finally, the lignin content was measured using the acid-insoluble (Klason) lignin method as described in TAPPI T 222 om-11.

Scanning electron microscopy

Scanning electron microscopy (SEM) was conducted using an INSPECT S50 microscope (FEI Company) operating under high vacuum conditions. Prior to examination, all fiber samples were sputter-coated with a layer of gold in order to ensure electrical conductivity. The analysis was performed at magnification levels ranging from 100 to 4000x. The operating parameters were set as follows: an aperture size of 3.5 to 5 µm, a working distance of 10 mm, and an accelerating voltage of 5-7 kV.

Assessing the fiber-cement boards

Physical and mechanical evaluation

The physical properties of the fiber-cement boards were evaluated as follows. The moisture content was measured for each board (N=10) using the gravimetric method as described in ASTM C1185-08 (2016). The density of each board was determined (N=6) while following DIN EN ISO 52361:1965-04 (2004b). Additionally, the water absorption capacity and corresponding volumetric swelling were measured (N=5) in accordance with DIN EN ISO 52364:2011 (2004c).

The mechanical properties evaluated included the MOR, determined via static bending tests (N=3) as per DIN EN ISO 52362:2011 (2004a), and the thickness reduction under compression (N=4), tested in accordance with ASTM-C1186-22 (2022).

Fourier-transform infrared spectroscopy

The fiber-cement board samples were analyzed by Fourier-transform infrared (FTIR) spectroscopy using a BRUKER Alpha II spectrometer equipped with an ECO-ATR accessory. Each sample was scanned over a wavenumber range of 4000 to 400 cm^{-1}, at a resolution of 4 cm^{-1}. For each measurement, multiple scans were averaged to improve the signal-to-noise ratio. Throughout the analysis, ambient temperature and humidity were carefully controlled.

RESULTS

Fibers

Chemical characterization

The chemical composition of both NT and T fibers was quantified, including the percentages of alcohol-soluble extractives, water-soluble extractives, holocellulose, lignin, ash, and moisture.

When ethanol was used as the solvent, the extractives content was 1.25% for the NT fibers and 1.27% for the T fibers. The alkaline pretreatment with the 10% NaOH solution led to a notable decrease in holocellulose content, which dropped from 73.77% (NT) to 68.45% (T). In contrast, the lignin content remained relatively unchanged at 30.68% (NT) and 30.53% (T). The ash content was significantly higher in pretreated fibers, measuring 1.30% compared to 0.93% (NT). Additionally, the alkaline pretreatment reduced the moisture content of the fibers.

Scanning electron microscopy

Representative SEM images of the NT and T fibers, captured at magnifications of 400 and 800x, are presented in Figure 2.

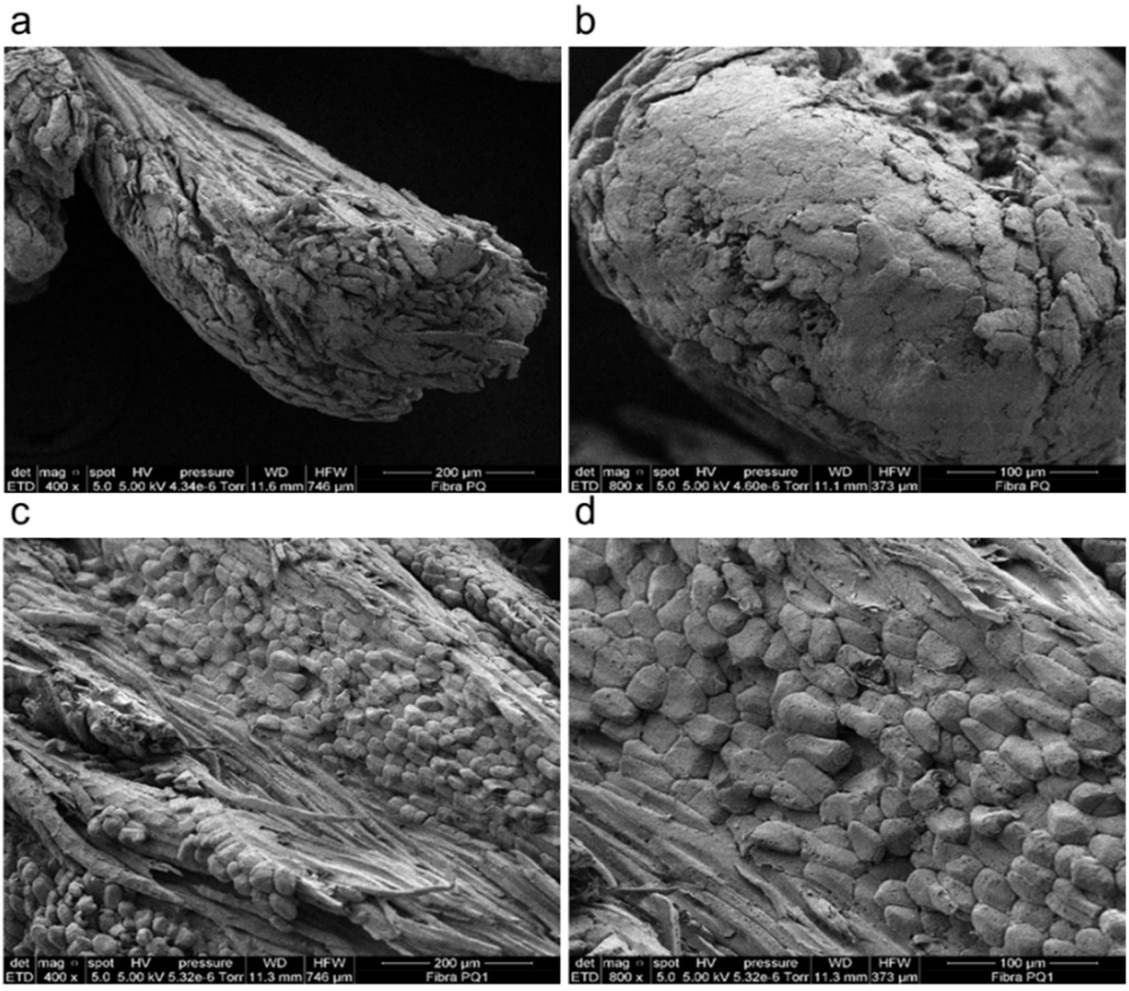

Figure 2. a) SEM image of NT fibers at 400x magnification, b) SEM image of NT fibers at 800x, c) SEM image of T fibers at 400x, d) SEM image of T fibers at 800x.

A microstructural analysis revealed that the fibrillar elements exhibited a slenderness ratio greater than 1, confirming their characteristic fibrous morphology. The fibers were fractionated by size into five distinct categories using a Bauer-McNett classifier. The classification results, including the corresponding sieve numbers and the nominal size ranges of the retained fiber fractions, are detailed in Table 1, following the TAPPI T 233 cm-06 standard (2006).

As shown in Table 1, most of the NT fibers (64.15%) were classified within the 0.297-0.595 mm length fraction. In contrast, the T fibers were predominantly longer, with 49.66% in the fraction exceeding 0.595 mm. This distribution indicates that the alkaline pretreatment resulted in a higher proportion of longer fibers compared to the untreated sample.

Table 1. Bauer-McNett fiber classification of fibers without pretreatment (NT) and with an alkaline pretreatment (T)

Sieve (mesh)	Longitude (mm)	NT (%)	T (%)
> +30	> 0.595	35.01	49.66
−30/ + 50	0.297–0.595	64.15	16.62
−50 /+100	0.149–0.297	0.22	8.61
−100/+200	0.074–0.149	0.11	8.03
<−200	<0.074	0.51	17.08

Assessment of the fiber-cement boards

Physical and mechanical evaluation

The results of the physical and mechanical evaluations are presented in Figure 3. The data indicate a positive correlation between fiber content and water retention in the fiber-cement boards. Specifically, the moisture content increased with higher fiber percentages.

For the boards reinforced with NT fibers, the moisture content was 7.19% at a 3% fiber concentration, rising to 7.42% and 7.79% for samples with 6 and 9% fiber, respectively. A similar trend was observed for the T fibers, with moisture contents of 7.19, 7.51, and 7.95% at fiber concentrations of 3, 6, and 9%. The alkaline pretreatment with NaOH did not result in a significantly different moisture content in comparison with the untreated fibers.

Conversely, the mechanical properties, specifically the thickness reduction under compression and the MOR under static bending, exhibited a decreasing trend with increasing fiber content for both the NT and T fiber-reinforced boards. The highest average flexural strength (MOR) was observed in the pure cement boards (0% fiber), with a value of 81.15 $kg.cm^{-2}$. The boards containing 3% fiber demonstrated intermediate MOR values, ranging from 63.81 to 65.38 $kg.cm^{-2}$, with no statistically significant difference observed between NT and T fibers at this concentration. The lowest MOR values, which were significantly lower, were recorded for boards with 9% fiber, averaging between 46.61 and 47.22 $kg.cm^{-2}$. This represents a reduction of approximately 50% compared to the pure cement boards. This decline in flexural performance with higher fiber loading is likely attributable to an inadequate matrix-fiber adhesion, resulting in poor stress transfer and stress concentration at the interface.

Scanning electron microscopy

Figure 4 presents representative SEM images of the fracture surfaces of the boards reinforced with 3, 6, and 9% NT and T fibers.

At a higher magnification (2000x), the board with 3% NT fibers (Figure 4a) exhibits a relatively compact matrix with localized regions of fiber aggregation (highlighted in red circles). The fiber-matrix interface shows partial cohesion, but some fibers appear to be poorly integrated, resulting in an overall acceptable distribution, albeit with zones of weak interfacial adhesion. Furthermore, the microstructure reveals delamination, microcracking, and an increased porosity. These microstructural features are critical for understanding potential pathways for water ingress and environmental degradation, which can compromise the long-term durability of the material (Kurpińska *et al*., 2022).

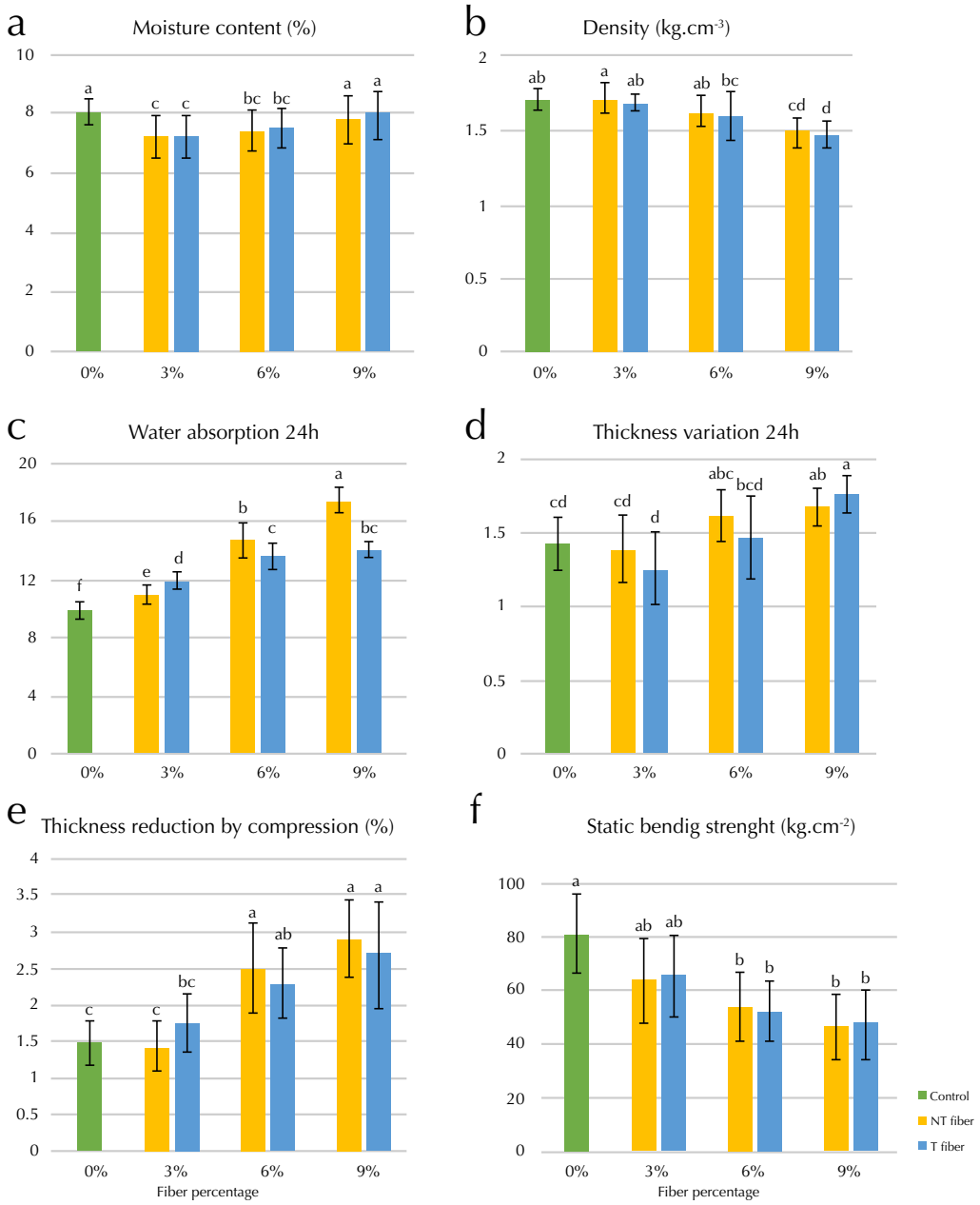

Figure 3. Physical and mechanical properties of the fiber-cement boards without pretreatment (NT) and with an alkaline pretreatment (T). a) Moisture content (%); b) density g.cm^{-3}; c) water absorption over 24 h (%); d) water variation over 24 h (%); e) thickness reduction under compression (%); f) static flexural strength in (kg.cm^{-2}).

Fourier-transformed infrared spectroscopy

Figure 5 presents the FTIR spectra of the fiber-reinforced boards. The profiles for the samples containing NT fibers (Figure 5a) and T fibers (Figure 5b) exhibit notable similarity.

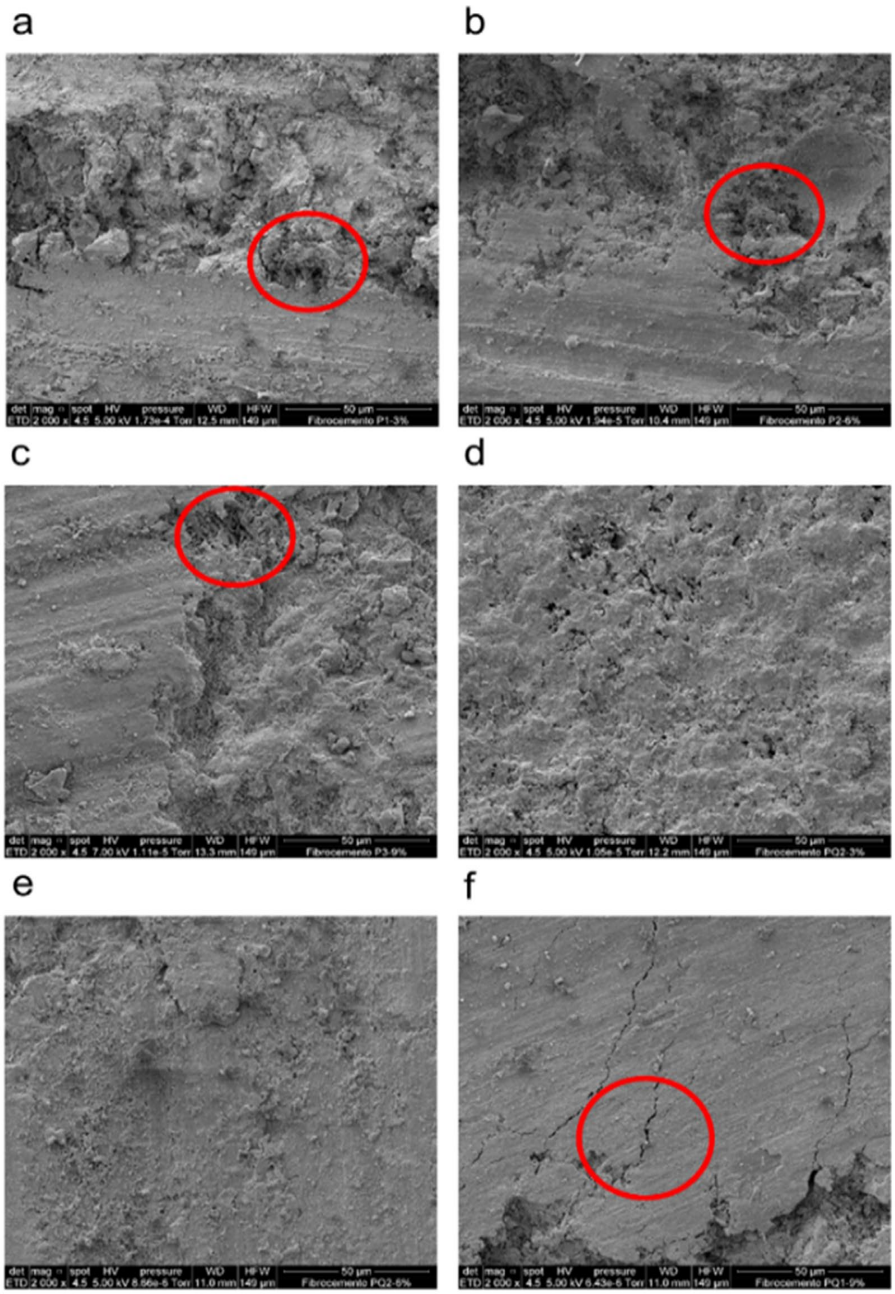

Figure 4. SEM images of the fiber-cement boards: a) NT at 3%, 2000x magnification; b) NT at 6%, 2000x; c) NT at 9%, 2000x; d) T at 3%, 2000; e) T at 6%, 2000x; f) T at 9%, 2000x.

A characteristic band associated with cement hydration was observed in all samples within the range of 800-1000 cm^{-1}, corresponding to the Si–O stretching vibration in the silicate chains of calcium silicate hydrate (C-S-H). Additionally, a band in the range of 1400-1480 cm^{-1}, attributed to the asymmetric stretching vibration of carbonate ions (CO_3^{2-}), was identified in all compositions. This band is typical of carbonation products in hydrated cement systems and is primarily associated with calcium carbonate ($CaCO_3$). The presence of these bands was consistent across all fiber types and loading levels (3, 6, and 9% content for both NT and T fibers) (Yusuf, 2023).

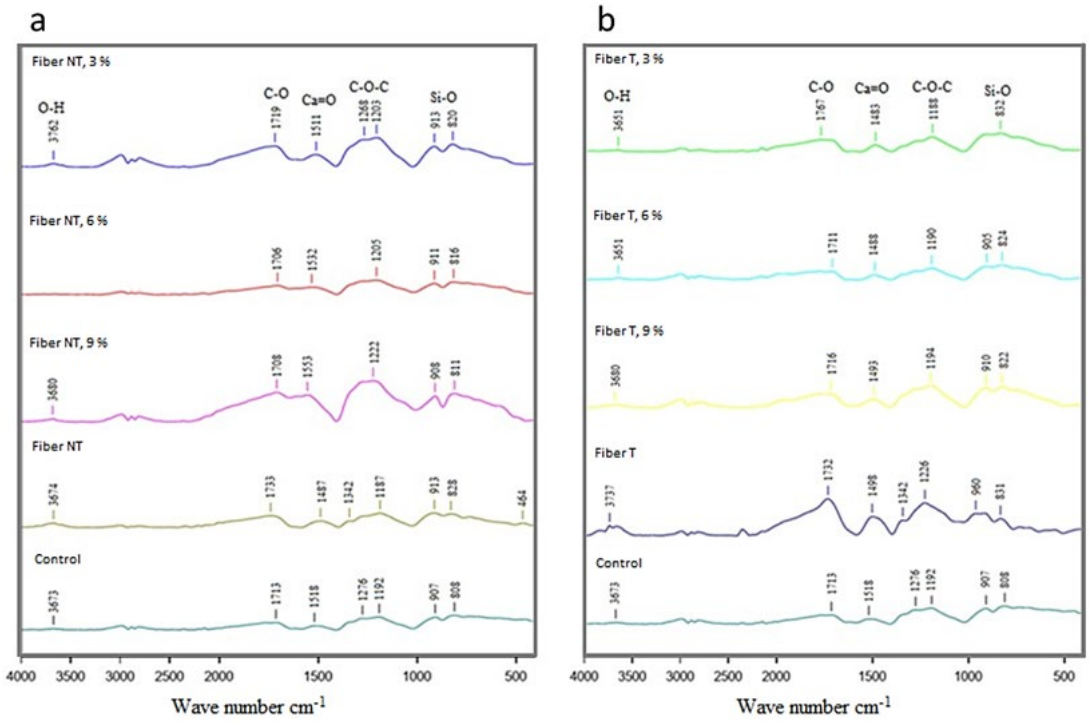

Figure 5. Fourier-transformed infrared spectroscopy analysis of a) the NT fiberboards and b) the T fiberboards

DISCUSSION

Fibers

Chemical characterization

An alkaline pretreatment with NaOH was employed to reduce the hemicellulose content of the samples. This process is advantageous, as soluble extractives such as sugars and starches can inhibit cement hydration and delay setting (Llerena, 2014). Compared to ethanol extraction, hot water extraction yielded a higher proportion of soluble compounds from both fiber types, indicating its greater efficacy in removing extractives. This result is consistent with findings reported by Karaseva *et al*. (2019) for chestnut pericarp fibers. When ethanol was used as the solvent, the extractives content was 1.25% for the NT fibers and 1.27% for the T fibers. This negligible difference indicates that the alkaline pretreatment did not significantly affect the concentration of ethanol-soluble compounds, which is consistent with prior research (Teixeira *et al*., 2020). It is generally accepted that the total extractive content in fibers should not exceed 2.25% for optimal compatibility with cement. Extractives such as waxes, fats, and phenolic compounds can impair adhesion at the fiber-matrix interface. Their hydrophobic nature inhibits bonding with the hydrophilic cementitious binder, forming a barrier that reduces the stress transfer efficiency (Fernández-Carrasco *et al*., 2014). Furthermore, water-soluble extractives like sugars, tannins, and colorants can interfere with cement hydration kinetics, delaying setting time and compromising the development of mechanical properties (Laverde *et al*., 2022). An elevated extractives content may also promote microbial growth, leading to the biological degradation of the fibers and a consequent reduction in the long-term durability of the composite (Mohr *et al*., 2006).

The holocellulose content of the fibers, ranging from 68.45 to 73.77%, falls within the typical range reported for other plant fibers (Cipra Rodriguez *et al*., 2022; ÇitlaciFci *et al*., 2022; Córdova *et al*., 2020). However, the pretreatment with the 10% NaOH solution significantly reduced the holocellulose content from 73.77% (NT) to 68.45% (T). This reduction can be attributed to the degradation of holocellulose by sodium hydroxide, which hydrolyzes low-molecular-weight sugars and amorphous constituents (Wang *et al*., 2014). A high holocellulose content, primarily comprising structural cellulose with linear chains and high crystallinity, is desirable since it enhances fiber rigidity and mechanical resistance. Furthermore, it facilitates efficient stress transfer from the cement matrix to the fibers, a key advantage over reinforcements with lower holocellulose content (Hincapié Rojas *et al*., 2020). Conversely, low holocellulose percentages indicate a reduced potential for structural reinforcement, an inferior load transfer efficiency, and a diminished durability in the alkaline environment of cement matrices (Çavdar *et al*., 2022). Consequently, the observed reduction in the holocellulose content of the T fibers is expected to adversely affect the mechanical performance of the composite material.

The lignin content for both fiber types was approximately 30%, which lies within the typical range for natural fibers. The specific values obtained were 30.68% for NT fibers and 30.53% for T fibers. Although the NaOH pretreatment does not directly degrade lignin, it can solubilize and modify it, thereby reducing its cement-retarding properties (Ferraz *et al*., 2020). Lignin contributes to fiber rigidity and mechanical resistance while acting as a protective barrier against environmental degradation (Mohr *et al*., 2006). It also reduces fiber hydrophilicity, decreasing moisture absorption and improving dimensional stability in fiber-cement composites (Teixeira *et al*., 2020) However, an excessive lignin content may compromise fiber-matrix adhesion due to its lower chemical compatibility with the hydrophilic cement matrix when compared to cellulose (Fernández-Carrasco *et al*., 2014). According to Wei and Meyer (2016), a higher cellulose-to-lignin ratio is desirable for optimizing the mechanical performance of fiber-cement composites. Furthermore, the stability of lignin within the cement matrix is an indicator of fiber durability, as its degradation can signal long-term composite vulnerability (Chen *et al*., 2022).

In summary, the presence of both holocellulose and lignin is critical for achieving optimal mechanical properties and ensuring the long-term durability of fiber–cement composites.

The ash content was significantly higher in T fibers (1.30%) than in their NT counterparts (0.93%). This increase is attributed to the alkaline pretreatment, which removes organic impurities and combustible material, thereby concentrating inorganic constituents and resulting in a higher residual ash content following combustion (Kandel *et al*., 2022). We observed a notable difference in moisture content between the NT fibers (8.33%) and the T fibers (4.18%). This reduction in moisture content following the alkaline pretreatment is likely due to the removal of hydrophilic components, such as hemicelluloses, from the fiber surface, as reported in previous studies (Fernández-Carrasco *et al*., 2014). Consequently, it is reasonable to conclude that the alkaline pretreatment not only enhances the interaction with the cement matrix but also lowers the hygroscopicity of the chestnut fibers by diminishing their moisture content. This effect is beneficial for their use as reinforcement in fiber-cement composites, wherein the goal is to regulate water absorption.

Scanning electron microscopy

Notably, the NT fibers exhibit clustered and compact cells, whereas the T fibers, viewed transversely, display plant cells that are more distinct and separated because of the alkaline treatment. The SEM images of the NT

fibers (Figures 2a and 2b) reveal a surface with layers or flakes peeling at the fiber ends, suggesting potential fractures in the cell wall. Figure 3a shows a 400x micrograph of the NT fibers, displaying a fibrous bundle with an elongated, compact structure, characterized by a rough or laminated texture associated with the presence of lignin. In addition, the densely stacked strata contribute to the flow flexibility of the fibers (Wei & Meyer, 2015). The 800x micrograph of the NT fibers (Figure 2b) shows their structure is shown in finer detail, with a more pronounced and fractured texture, a scaly look, and visible wear, along with porous areas that are a part of the untreated fiber's natural texture (Choi & Choi, 2021). The NT fibers do not exhibit significant inhomogeneity or large impurities, which is advantageous for reinforcement applications (Sonego *et al*., 2021).

Figures 2c and 2d provide information on the T fibers, highlighting a greater uniformity in cell alignment and a more fibrous yet tapered appearance. This observation can be attributed to the alkaline pretreatment, which partially compromises the integrity of the cell walls, enhancing the fibers' flexibility. This modification considerably improves their adhesion and compatibility with the cementitious matrix (Wei & Meyer, 2015). The 800x SEM image of the T fibers (Figure 2d) reveals a smoother surface, a typical outcome of alkaline treatments that stems from the removal of impurities, yielding a more defined cellular structure (Sonego *et al*., 2019). Moreover, the clear cellular differentiation suggests that the treatment partially eliminated non-cellulosic substances, resulting in a more homogeneous and defined fiber. This enhanced morphology is likely to improve the fiber's performance under mechanical stress when used as reinforcement material in composites.

In general, the NT fibers exhibit shorter lengths and smaller diameters compared to the T fibers. This notable variation in size and shape between the two fiber types is due to the fact that the T fibers used in board production were subjected to a sieving process. During this process, the fibers retained on the 40-mesh sieve (400 µm) were selected. The NT fibers did not undergo this additional processing step, so they exhibited greater heterogeneity in their morphological properties.

According to the results, that the fibers had an average length ranging from 167 to 184 µm, with coefficients of variation between 12 and 30%, suggesting considerable variability in length. Furthermore, the average diameters ranged from 0.0025 to 0.0031 mm, also exhibiting substantial variability, as reflected by coefficients of variation of 29 to 45%. The length-to-diameter (aspect) ratios, or slenderness values, were generally greater than 65 on average, indicating a moderately proportional relationship between length and width. However, the slenderness also showed high variability. Notably, the average value is comparable to the slenderness index of other natural fibers (Nagaraja Ganesh *et al*., 2023).

Assessment of the fiber-cement boards

Physical and mechanical evaluations

Lilargem *et al*. (2022) also reported an increased moisture content in cementitious composites after the incorporation of various natural fibers, which can be attributed to the hydrophilic nature of lignocellulosic fibers. It is important to note that comparisons with other studies were qualitative but revealed consistent trends regarding the effect of fibers on moisture retention. The water absorption after 24 h for fiber-cement samples containing 3, 6, and 9% of both NT and T fibers indicated that higher fiber contents resulted in greater water absorption.

The samples with 9% fiber exhibited the highest absorption levels. This trend is explained by the inherent hydrophilicity and porosity of natural fibers, which promote water penetration and retention within the composite. The alkaline pretreatment removed surface impurities, such as waxes and oils, thereby exposing polar groups more extensively and slightly enhancing the hydrophilic properties of the fibers. As a result, the pretreated fiber samples showed higher absorption compared to untreated samples with the same fiber content. These findings are consistent with those reported in previous studies (Çavdar *et al*., 2022; Martinelli *et al*., 2023), particularly concerning the increased water absorption observed in cementitious composites reinforced with natural fibers.

The density measurements of the fiber-cement boards indicated that increased fiber content resulted in reduced sample density for both fiber types. The samples containing 9% fiber exhibited the lowest density values. This inverse relationship between fiber content and density can be attributed to the lower density of the plant fibers when compared to that of Portland cement, the primary constituent of the composite matrix. Therefore, an increase in the fiber proportion was expected to result in decreased board density (Tonoli *et al*., 2009). This finding aligns with previous studies: Teixeira *et al*. (2020) reported similar outcomes when substituting asbestos fibers with natural fibers in fiber-cement composites, while Gamarra *et al*. (2024) observed density reductions in cementitious materials reinforced with various plant fibers.

As the fiber content increases, the thickness variation of the boards also tends to escalate. Specifically, at a 3% NT fiber content, the average thickness was 1.39 mm, compared to 1.24 mm for T fiber. At 6% fiber, the thickness increased to 1.60 mm for NT fibers and 1.45 mm for T fibers. Finally, at 9%, the thickness reached 1.66 mm for NT and 1.75 mm for T. Samples with 9% T fiber exhibited the greatest variation.

This increase in thickness with higher fiber content can be attributed to the hygroscopic and porous nature of natural fibers, which absorb water and subsequently swell. A greater proportion of fibers leads to increased water uptake and, consequently, more pronounced swelling. The alkaline pretreatment partially modifies the fiber structure, enhancing its hydrophilicity and potentially amplifying this swelling behavior, leading to more marked thickness variations in treated fiber-cement composites(Suwan *et al*., 2022). The reduction in thickness under compression also increased with a higher fiber content. The smallest reductions were observed in samples without fiber and in those containing 3% fiber, while the samples with 6 and 9% fiber exhibited progressively greater reductions. The results of Kruskal-Wallis tests confirmed the statistically significant differences in thickness reduction across samples with different fiber contents, regardless of fiber pretreatment. The samples with 6 and 9% fiber content showed the most pronounced reduction.

Consistent with previous findings, the board density decreased as the fiber content increased, which inversely affected mechanical properties such as the resistance to compression. Higher porosity within the material—resulting from greater fiber incorporation—facilitates compaction under compressive loads (Sales *et al*., 2022). In a similar research work, Gamarra *et al*. (2024) explained that the impact of organic aggregates (lignocellulosic fibers) on mechanical compression is contingent on the quantity used in board formation.

As the fiber content increases, so does the interaction zone, thereby introducing more potential failure points where stress can concentrate, weakening the material under load (Tonoli *et al*., 2009). According to the DIN

EN ISO 52362:1965-04 standard (2008), fiber-cement boards with a thickness of 15 mm should have a minimum bending resistance of 17 kg.cm^{-2}, which is surpassed in this study, with the best performance recorded in compounds containing 3% *Bertholletia excelsa* mesocarp fiber.

Scanning electron microscopy

The microstructure exhibits no significant cracking, suggesting that the fibers do not introduce major discontinuities in the cement matrix. In the board with 6% NT fibers (Figure 4b), an increase in fiber clustering was observed, indicating a less uniform dispersion and a higher porosity compared to the 3% NT fiber board (Figure 4a). This implies an inferior fiber-matrix compatibility (Kurpińska *et al*., 2022), which can adversely affect mechanical performance and flexural strength. Reduced fiber-matrix contact in certain regions may compromise stress transfer efficiency. Figure 4c shows a sample with 9% NT fibers, where pronounced fiber clustering has led to the formation of voids and channels within the matrix, further disrupting its homogeneity. This suggests that the fiber content may exceed the capacity of the matrix for effective integration, resulting in weak zones and an increased propensity for microcracking or premature failure under stress. Increased surface roughness and initial fractures further diminish the internal cohesion of the composite.

The 2000x SEM images of the board with 3% T fibers (Figure 4d) demonstrated a more uniform microstructure, with improved adhesion between the fiber and the matrix, minimizing clusters and porosity, with no signs of cracking. This finding suggested a uniform contribution to the structural integrity, creating no weak points (Ferraz *et al*., 2020) and enhancing mechanical performance. The board with 6% T fibers (Figure 4e) remained consistent, showing a better fiber-cement matrix integration, with no cracks or voids. It also exhibited small pores that were uniformly distributed, indicating a good fiber-cement compatibility (Ferraz *et al*., 2020), possibly due to the soda (NaOH) treatment. However, the board containing 9% T fibers (Figure 4f) showed cracks, suggesting that, although the treatment improved the dispersion, the matrix continued to undergo excessive stress at a 9% T fiber concentration, with microcracks indicating fiber-induced weak points due to saturation, which affected the board's mechanical properties (Rocco & Elices, 2009). When compared to the 3% NT fiberboard (Figure 4c), fewer fiber clusters were present, but the cracking indicated that the fiber content remains a limiting factor for material strength.

Overall, the soda treatment enhanced the fiber-matrix integration, particularly in boards produced with a 3 and 6% T fiber content, reducing clusters and porosity. However, the boards made with 9% NT and T fiber displayed signs of brittleness with cracks that could impair mechanical performance. In NT fiberboards, the increased fiber content created clusters and matrix defects, suggesting that better adhesion may reduce mechanical resistance. Thus, the optimal fiber content appears to be 3-6%, as the product showed a more uniform microstructure without any significant cracks.

Fourier-transform infrared spectroscopy

In the spectra, O–H appeared in the 3400-3650 cm^{-1} range and was related to hydrogen bonds (Arango-Perez *et al*., 2023; Zavaleta-Cavero *et al*., 2024). For fiber-cement, this band is associated with the O–H bond

produced by Portlandite ($Ca(OH)^2$), which is a precursor to the components of hydrated cement, such as hydrated tricalcium silicate (C3SH), hydrated dicalcium silicate (C2SH), hydrated tricalcium aluminate (C3AH), and tetracyclic ferroaluminate (C4AF) (Chakraborty *et al*., 2013).

The aforementioned spectra displayed similar peaks, with more pronounced peaks in the boards produced with NT fiber when compared with their T counterparts, in relation to the functional groups tied to holocellulose and lignin. This can be attributed to the dissolution of lignocellulosic components under the alkaline treatment. When the T fibers were treated with NaOH, components like lignin, hemicellulose, and short, amorphous chain cellulose were removed.

CONCLUSIONS

The fibers extracted from the mesocarp of *B. excelsa* were found to be well-suited for manufacturing fiber-cement boards, as their characteristics meet the standards of ASTM-C1186-22 (2022). Fiber-mesocarp chestnut boards pretreated with 3% NaOH exhibited superior physical-mechanical properties. The chemical composition of these fibers supported their use as a reinforcement material in fiber-cement board production. When examining the different fiber percentage compositions of the boards, a noticeable direct correlation with the moisture content and density was observed.

ACKNOWLEDGEMENTS

The authors acknowledge the support provided by the Forest Chemistry Laboratory, the Pulp and Paper Laboratory, the technicians Marco Panduro and Enrique Cabrera, and Prof. Deysi Guzmán. They also would like to thank to the Research Vice-Principal's Office of for the support provided through ENAGO in the English edition of this document .

CONFLICTS OF INTEREST

The authors declare no conflicts of interest with respect to the research, authorship, and publication of this paper.

AUTHORSHIP CONTRIBUTIONS

C. M. S.: data curation, Formal Analysis, Investigation, Methodology, Software, Validation, Writing (original draft). H. E. G. M.: conceptualization, funding acquisition, supervision, project administration, resources, methodology. J. G. B.: formal analysis, writing (review & editing). A. J. C. O.: conceptualization, supervision, methodology, writing (original draft, review, & editing).

REFERENCES

American Society for Testing and Materials (ASTM) (2022). *Standard Test Method for Chemical Analysis of Wood Charcoal*. ASTM.

American Society for Testing and Materials (ASTM) (2016). *ASTM C1185-08 Standard Test Methods for Sampling and Testing Non-Asbestos Fiber-Cement Flat Sheet, Roofing and Siding Shingles, and Clapboards*. ASTM.

American Society for Testing and Materials (ASTM) (2022). *ASTM-C1186-22 Standard Specification for Flat Fiber-Cement Sheets* (Nos. C1186-22). ASTM.

Arango-Pérez, S. A., Gonzales-Mora, H. E., Ponce-Álvarez, S. P., Gutarra-Espinoza, A. A., & Cárdenas-Oscanoa, A. J. (2023). Assessment of cellulose nanofibers from bolaina blanca wood obtained at three shaft heights. *Maderas-Ciencia y Tecnología*, *26*, e1824. https://doi.org/10.22320/s0718221x/2024.18

Atúncar Vilela, W. B., Gonzales Mora, H. E., Arango, S., & Cárdenas-Oscanoa, A. J. (2024). Elaboración de papel con fibra virgen y reciclada reforzada con celulosa nanofibrilada de Guadua angustifolia. *Colombia Forestal*, *27*(2), e20917. https://doi.org/10.14483/2256201X.20917

Campello, E. F., Pereira, M. V., Darwish, F. A., & Ghavami, K. (2016). On the fatigue behavior of bamboo pulp reinforced cementitious composites. *Procedia Structural Integrity*, *2*, 2929-2935. https://doi.org/10.1016/j.prostr.2016.06.366

Çavdar, A. D., Yel, H., & Torun, S. B. (2022). Microcrystalline cellulose addition effects on the properties of wood cement boards. *Journal of Building Engineering*, *48*, 103975. https://doi.org/10.1016/j.jobe.2021.103975

Chakraborty, S., Kundu, S. P., Roy, A., Adhikari, B., & Majumder, S. B. (2013). Effect of jute as fiber reinforcement controlling the hydration characteristics of cement matrix. *Industrial & Engineering Chemistry Research*, *52*(3), 1252-1260. https://doi.org/10.1021/ie300607r

Chen, Y., Li, Y., Zhang, C., Qi, H., & Hubbe, M. A. (2022). Holocellulosic fibers and nanofibrils using peracetic acid pulping and sulfamic acid esterification. *Carbohydrate Polymers*, *295*, 119902. https://doi.org/10.1016/j.carbpol.2022.119902

Choi, H., & Choi, Y. C. (2021). Setting characteristics of natural cellulose fiber reinforced cement composite. *Construction and Building Materials*, *271*, 121910. https://doi.org/10.1016/j.conbuildmat.2020.121910

Cipra Rodriguez, J. A., Gonzales Mora, H. E., & Cárdenas Oscanoa, A. J. (2022). Characterization of MDF produced with bolaina (*Guazuma crinita* Mart.) wood residues from plantation. *Madera y Bosques*, *28*(3), e2832433. https://doi.org/10.21829/myb.2022.2832433

Çitlacifci, H., Kiliç Pekgözlü, A., & Gülsoy, S. K. (2022). Characterization of cheestnut shell. *Bartın University International Journal of Natural and Applied Sciences, 5*(2), 145-150. https://doi.org/10.55930/jonas.1207620

Córdova Contreras, A. R., Cárdenas Oscanoa, A. J., & Gonzáles Mora, H. E. (2020). Physical and mechanical characterization of *Guazuma crinita* Mart. composites based on virgin polypropylene. *Revista Mexicana de Ciencias Forestales*, *11*(57), 1-28. https://doi.org/10.29298/rmcf.v11i57.621

Correia, V. C., Santos, S. F., Savastano Jr, H., & John, V. M. (2018). Utilization of vegetable fibers for production of reinforced cementitious materials. *RILEM Technical Letters*, *2*, 145-154. https://doi.org/10.21809/rilemtechlett.2017.48

Deutsches Institut für Normung (DIN) (1965a). *Testing of wood chipboards; bending test, determination of bending strength (DIN 52362-1:1965-04)* [Withdrawn standard]. Beuth Verlag, DIN.

Deutsches Institut für Normung (DIN) (1965b). *Testing of wood chipboards; determination of dimensions, raw density and moisture content (DIN 52361:1965-04)* [Withdrawn standard]. Beuth Verlag, DIN.

Deutsches Institut für Normung (DIN) (1965c). *Testing of wood chipboards; determination of variation in thickness due to moisture (DIN 52364:1965-04)* [Withdrawn standard]. Beuth Verlag, DIN.

do Amaral, L. M., Rodrigues, C. D. S., & Poggiali, F. S. J. (2022). Hornification on vegetable fibers to improve fiber-cement composites: A critical review. *Journal of Building Engineering*, *48*, 103947. https://doi.org/10.1016/j.jobe.2021.103947

Fernández-Carrasco, L., Claramunt, J., & Ardanuy, M. (2014). Autoclaved cellulose fibre reinforced cement: Effects of silica fume. *Construction and Building Materials*, *66*, 138-145. https://doi.org/10.1016/j.conbuildmat.2014.05.050

Ferraz, P. F. P., Mendes, R. F., Marin, D. B., Paes, J. L., Cecchin, D., & Barbari, M. (2020). Agricultural Residues of Lignocellulosic Materials in Cement Composites. *Applied Sciences*, *10*(22), 8019. https://doi.org/10.3390/app10228019

Fonseca, C. S., Silva, M. F., Mendes, R. F., Hein, P. R. G., Zangiacomo, A. L., Savastano, H., & Tonoli, G. H. D. (2019). Jute fibers and micro/nanofibrils as reinforcement in extruded fiber-cement composites. *Construction and Building Materials*, *211*, 517-527. https://doi.org/10.1016/j.conbuildmat.2019.03.236

Gamarra-Romero, L. F., Gonzales Mora, H. E., Cipra-Rodríguez, J. A., & Cárdenas-Oscanoa, A. J. (2024). Effect of adding oil palm (*Elaeis guineensis* Jacq.) mesocarp fibers to cement composites. *Colombia Forestal*, *27*(2), e21457. https://doi.org/10.14483/2256201X.21457

Hasan, K. M. F., Horváth, P. G., & Alpár, T. (2022). Lignocellulosic fiber cement compatibility: A state of the art review. *Journal of Natural Fibers*, *19*(13), 5409-5434. https://doi.org/10.1080/15440478.2021.1875380

Hincapié Rojas, D. F., Pineda-Gómez, P., & Guapacha-Flores, J. F. (2020). Effect of silica nanoparticles on the mechanical and physical properties of fibercement boards. *Journal of Building Engineering*, *31*, 101332. https://doi.org/10.1016/j.jobe.2020.101332

Kandel, K. P., Adhikari, M., Kharel, M., Aryal, G. M., Pandeya, S., Joshi, M. K., Dahal, B., Gautam, B., & Neupane, B. B. (2022). Comparative study on material properties of wood-ash alkali and commercial alkali treated Sterculia fiber. *Cellulose*, *29*(10), 5913-5922. https://doi.org/10.1007/s10570-022-04610-w

Karaseva, V., Bergeret, A., Lacoste, C., Ferry, L., & Fulcrand, H. (2019). Influence of extraction conditions on chemical composition and thermal properties of chestnut wood extracts as tannin feedstock. *ACS Sustainable Chemistry & Engineering*, *7*(20), 17047-17054. https://doi.org/10.1021/acssuschemeng.9b03000

Kurpińska, M., Pawelska-Mazur, M., Gu, Y., & Kurpiński, F. (2022). The impact of natural fibers' characteristics on mechanical properties of the cement composites. *Scientific Reports*, *12*(1), 20565. https://doi.org/10.1038/s41598-022-25085-6

Laverde, V., Marin, A., Benjumea, J. M., & Rincón Ortiz, M. (2022). Use of vegetable fibers as reinforcements in cement-matrix composite materials: A review. *Construction and Building Materials*, *340*, 127729. https://doi.org/10.1016/j.conbuildmat.2022.127729

Lilargem Rocha, D., Tambara Júnior, L., Marvila, M., Pereira, E., Souza, D., & de Azevedo, A. (2022). A Review of the use of natural fibers in cement composites: Concepts, applications and Brazilian history. *Polymers*, *14*(10), 2043. https://doi.org/10.3390/polym14102043

Llerena, A. (2014). *Estudio de compuestos cementíceos reforzados con fibras vegetales: Evaluación previa del comportamiento de un panel de cemento blanco con adición de meta-caolín reforzado con un textil no-tejido de fibras largas de lino y cáñamo* [Master's thesis, Universitat Politècnica de Catalunya]. http://hdl.handle.net/2099.1/25365

Mármol, G., & Savastano, H. (2017). Study of the degradation of non-conventional MgO-SiO2 cement reinforced with lignocellulosic fibers. *Cement and Concrete Composites*, *80*, 258-267. https://doi.org/10.1016/j.cemconcomp.2017.03.015

Martinelli, F. R. B., Ribeiro, F. R. C., Marvila, M. T., Monteiro, S. N., Filho, F. D. C. G., & Azevedo, A. R. G. D. (2023). A Review of the use of coconut fiber in cement composites. *Polymers*, *15*(5), 1309. https://doi.org/10.3390/polym15051309

Mohr, B. J., Biernacki, J. J., & Kurtis, K. E. (2006). Microstructural and chemical effects of wet/dry cycling on pulp fiber–cement composites. *Cement and Concrete Research*, *36*(7), 1240-1251. https://doi.org/10.1016/j.cemconres.2006.03.020

Nagaraja Ganesh, B., Rekha, B., Mohanavel, V., & Ganeshan, P. (2023). Exploring the Possibilities of Producing Pulp and Paper from Discarded Lignocellulosic Fibers. *Journal of Natural Fibers*, *20*(1), 2137618. https://doi.org/10.1080/15440478.2022.2137618

Petrechen, G., Arduin, M., & Ambrósio, J. (2019). Morphological Characterization of Brazil Nut Tree (*Bertholletia excelsa*) Fruit Pericarp. *Journal of Renewable Materials*, *7*(7), 683-692. https://doi.org/10.32604/jrm.2019.04588

Rocco, C. G., & Elices, M. (2009). Effect of aggregate shape on the mechanical properties of a simple concrete. *Engineering Fracture Mechanics*, *76*(2), 286-298. https://doi.org/10.1016/j.engfracmech.2008.10.010

Sales, S. L. T., Aldamia, F. J., Gonzaga, P. S., Montesclaros, A. J. S., & Lawagon, C. P. (2022). Properties of fiber cement boards influenced by BSCH (banana stem and corn husk) fibers and citric acid addition. *Key Engineering Materials*, *913*, 125-130. https://doi.org/10.4028/p-qv513a

Soares, C., Moura, E., Arenhardt, V., Deliza, E. E. V., & Pedro Filho, F. D. S. (2023). Biotechnology management in the Amazon and the production of polypropylene / Brazil nut shell fiber biocomposite. *Revista de Gestão e Secretariado, 14*(7), 10734-10748. https://doi.org/10.7769/gesec.v14i7.2424

Soltan, D. G., das Neves, P., Olvera, A., Savastano Junior, H., & Li, V. C. (2017). Introducing a curauá fiber reinforced cement-based composite with strain-hardening behavior. *Industrial Crops and Products*, *103*, 1-12. https://doi.org/10.1016/j.indcrop.2017.03.016

Sonego, M., Fleck, C., & Pessan, L. A. (2019). Mesocarp of Brazil nut (*Bertholletia excelsa*) as inspiration for new impact resistant materials. *Bioinspiration & Biomimetics*, *14*(5), 056002. https://doi.org/10.1088/1748-3190/ab2298

Sonego, M., Madia, M., Eder, M., Fleck, C., & Pessan, L. A. (2021). Microstructural features influencing the mechanical performance of the Brazil nut (*Bertholletia excelsa*) mesocarp. *Journal of the Mechanical Behavior of Biomedical Materials*, *116*, 104306. https://doi.org/10.1016/j.jmbbm.2020.104306

Suwan, T., Maichin, P., Fan, M., Jitsangiam, P., Tangchirapat, W., & Chindaprasirt, P. (2022). Influence of alkalinity on self-treatment process of natural fiber and properties of its geopolymeric composites. *Construction and Building Materials*, *316*, 125817. https://doi.org/10.1016/j.conbuildmat.2021.125817

Technical Association of the Pulp and Paper Industry (TAPPI) (2017). *Solvent Extractives of Wood and Pulp, Test Method T 204 cm-17*. TAPPI.

Technical Association of the Pulp and Paper Industry (TAPPI) (2022). *Water solubility of wood and pulp, Test Method T 207 cm-22*. TAPPI.

Technical Association of the Pulp and Paper Industry (TAPPI) (2006). *Fiber Length of Pulp by Classification, Test Method T 233 cm-06.* TAPPI.

Technical Association of the Pulp and Paper Industry (TAPPI) (2021). *Acid-insoluble lignin in wood and pulp, Test Method T 222 om-21*. TAPPI.

Technical Association of the Pulp and Paper Industry (TAPPI) (2015). *Holocellulose in wood (T 9 wd 75)*. TAPPI Press. TAPPI.

Teixeira, J. N., Silva, D. W., Vilela, A. P., Savastano Junior, H., de Siqueira Brandão Vaz, L. E. V., & Mendes, R. F. (2020). Lignocellulosic materials for fiber cement production. *Waste and Biomass Valorization*, *11*(5), 2193-2200. https://doi.org/10.1007/s12649-018-0536-y

Tonoli, G. H. D., Rodrigues Filho, U. P., Savastano, H., Bras, J., Belgacem, M. N., & Rocco Lahr, F. A. (2009). Cellulose modified fibres in cement based composites. *Composites Part A: Applied Science and Manufacturing*, *40*(12), 2046-2053. https://doi.org/10.1016/j.compositesa.2009.09.016

Wang, Y., Lindström, M. E., & Henriksson, G. (2014). Increased degradability of cellulose by dissolution in cold alkali. *BioResources*, *9*(4), 7566-7578. https://doi.org/10.15376/biores.9.4.7566-7578

Wei, J., & Meyer, C. (2015). Degradation mechanisms of natural fiber in the matrix of cement composites. *Cement and Concrete Research*, *73*, 1-16. https://doi.org/10.1016/j.cemconres.2015.02.019

Wei, J., & Meyer, C. (2016). Utilization of rice husk ash in green natural fiber-reinforced cement composites: Mitigating degradation of sisal fiber. *Cement and Concrete Research*, *81*, 94-111. https://doi.org/10.1016/j.cemconres.2015.12.001

Yusuf, M. O. (2023). Bond characterization in cementitious material binders using Fourier-transform infrared spectroscopy. *Applied Sciences*, *13*(5), 3353. https://doi.org/10.3390/app13053353

Zavaleta-Cavero, D. A., Chumpitaz-Príncipe, D. A., Gutarra-Espinoza, A. A., Cárdenas-Oscanoa, A. J., Gonzales-Mora, H. E., Quino-Favero, J. M., Gómez-Maldonado, D., Peresin, M. S., & Ponce-Álvarez, S. P. (2024). From Bolaina Blanca wood fibers to antimicrobial films: Characterization and application in the food industry using copper nanoparticles. *Journal of Natural Fibers*, *21*(1), 2431314. https://doi.org/10.1080/15440478.2024.2431314